

> REPLACE THIS LINE WITH YOUR MANUSCRIPT ID NUMBER (DOUBLE-CLICK HERE TO EDIT) <

Implementation of a Virtualized PMU in a CPC platform based on IEC61850 Sampled Values

Anibal Antonio Prada Hurtado, Mario Manana, Maria Teresa Villén Martínez, Miguel Ángel Olivan Monge, Eduardo Martinez Carrasco and Carlos Rodriguez del Castillo

Abstract— This paper presents the implementation of Phasor Measurement Units (PMUs) using IEC61850 Sampled Values (SV) in a Centralized Protection and Control (CPC) platform called EPICS platform. The SV-PMU microservice is developed and implemented via software on an EDGE Server. Two versions of the SV-PMU microservice were implemented and evaluated, the first one uses a two-cycle FIR filter, and the second one uses a one-cycle FIR filter. Both implementations use the signals generated by a Stand-Alone Merging Unit as input. The SV-PMU microservice performance is evaluated in the laboratory in both steady and transient states according to IEEE/IEC 60255-118-1:2018 standard. The evaluation tests were executed using a Real-Time Digital Simulator (RTDS). Two methods for the evaluation of the behaviour of the PMUs in terms of TVE, FE and RFE were implemented. The tests results demonstrate the microservice's compliance with the synchrophasor standards requirements in terms of TVE, FE, RFE and latency. Future improvements are required to warrantee the TVE values during 10 % rated current magnitude test. This implementation enhance the EPICS platform's capabilities as a CPC system in Digital Substations and to contribute to the deployment of Wide Area Monitoring, Protection, and Control (WAMPAC) systems in the power grid. This work includes the comparison of the behaviour of SV-PMU microservice with a commercial PMU to validate its real-world applicability.

Index Terms— IEC61850, Sampled Value, Phasor measurement units, Stand Alone Merging Unit, Centralized Protection and Control, Wide area measurements, Digital Substations.

I. INTRODUCTION

NOWADAYS, power systems are undergoing rapid changes in terms of grid operation, due to the need to meet greenhouse gas emission reduction targets by

This paragraph of the first footnote will contain the date on which you submitted your paper for review, which is populated by IEEE. This work was supported by the Edge Protection and Intelligent Control System (EPICS) Project of ELEWIT and has allowed the use of the EPICS platform for the development and implementation of the SV-PMU microservice. Banco Santander and Universidad de Cantabria partially supported Anibal Antonio Prada Hurtado's work within the industrial Doctorate program 2023 (BOC 224, 22nd November 2023). (Corresponding author: Anibal Antonio Prada Hurtado).

Anibal Antonio Prada Hurtado, Maria Teresa Villén Martínez, Miguel Ángel Olivan Monge and Eduardo Martinez Carrasco are with CIRCE Technology Centre, 50018 Zaragoza, Spain (aaprada@fcirce.es, mtvillen@fcirce.es, maolivan@fcirce.es, emartinez@fcirce.es).

Mario Manana is with Universidad de Cantabria, 39005 Santander, Spain (mario.manana@unican.es).

Carlos Rodriguez del Castillo is with Elewit (A company of Redeia), 28760 Madrid, Spain (calrodriguez@ree.es).

Digital Object Identifier XXXXXXXXXXXX

the year 2050. To achieve this goal, countries are executing plans for accelerated installation of renewable generation sources, thereby replacing fossil fuel-based generation sources. On the other hand, a digitization plan is also being implemented with the aim of saving construction and maintenance costs, as well as optimizing operation with the processing of large amounts of information using Big Data techniques and Artificial Intelligence that can work in times very close to real time.

The dynamics of the grid have been affected by the transition to renewable energy sources with power electronics interface device (PEID), as they have a different behaviour than that provided by synchronous generators. For example, effects have been observed in the behaviour of protections, and changes in frequency variations due to disturbances caused by the decrease in system inertia. For example in [1] and [2] are highlighted the issues related with the distance protections in electrical power systems with renewable generators with PEID and possible solutions are proposed. In [3], the behaviour in front of short-circuits associated with renewable generation with PEID is explained and is compared with the behaviour associated with the synchronous generators. The impact of renewable generation on grid inertia and frequency response of the Indian and European power systems is highlighted in [4] and [5]. The impact of inverted based generation on power system dynamics and short-circuits performance are highlighted in [6]. In [7] a method is proposed to estimate the maximum penetration level of renewable generation based on frequency stability constrains in power grids.

Traditionally, control centers have based their operation on measurements that are refreshed approximately every 1-4 seconds, supervised by a SCADA system. With this time resolution and information, it is not possible to execute algorithms that operate near real time. As an alternative to the above, the WAMPAC systems are presented, which can provide more accurate and time-synchronized information about the state and dynamics of the grid. A WAMPAC system use synchrophasor measurements generated by Phasor Measurement Units, which are capable of generating data up to every 8 ms (120 fps) or 16 ms (60 fps) in a 60 Hz Power System, or every 10 ms (100 fps) or 20 ms (50 fps) in a 50 Hz Power System (depending of the data rates available in the device), synchronized in time in compliance with IEEE/IEC 60255-118-1:2018 standards [8] [9] [10] [11]. More information about WAMPAC systems can be found in [12], where it is explained, in general, the basics of this kind of systems. Related with WAMPAC systems applications, in [13]

> REPLACE THIS LINE WITH YOUR MANUSCRIPT ID NUMBER (DOUBLE-CLICK HERE TO EDIT) <

is proposed an algorithm for islanding detection of distributed generation; a wide-area inter-area oscillation control in the Great Britain electrical power system is proposed in [14]; and different wide-area protection algorithms are described and proposed in [15] and [16].

Typically, conventional PMU needs to have secondary voltages and currents wired in order to work properly. In the process of digitalization of the substations, starting the measurements with Stand-Alone Merging Units (SAMU) or digital instrument transformers, it is natural for the evolution of PMUs to move towards the use of measurements based on IEC61850 SV [17] [18]. The IEEE/IEC 60255-118-1:2018 standard [8], in its Annex E, opens the door to this possibility and generally defines how it should operate and the evaluation criteria. Few commercial devices offer this capability as the described in [19] or the SV based distributed solutions detailed in [20]. In [21], a comparison of the behaviour between conventional PMU and the combination of commercial SAMU + SV based PMU is shown, concluding that this combination is feasible of its use in synchronized phasor measurements systems like WAMS or WAMPAC.

Some non-commercial implementations of PMUs based on IEC61850 SV, called *SV-PMU*, have been found in the literature. In [22], a preliminary study of measurement of synchrophasors with SAMUs is presented. During that study the *SV-PMU* was not implemented in hardware, and the comparison of the measurement results between a conventional PMU and the phasor estimation using the SVs collected are performed in a post-processing stage.

In [23] and [24], the *SV-PMU* is implemented in an embedded industrial controller (NI cRIO-9068) with Linux Real-Time OS and a re-configurable FPGA board. The authors explain that they detect some bottlenecks related to the behaviour of the ethernet communication ports when the host computer (NI PXIe 1062Q) is communicating with the controller. It is not possible to have more than one ethernet port active at a time. The scalability of the solution is not represented, the paper is focused on the implementation of a single *SV-PMU*.

As novelty, the present paper includes the following items:

- Proposes and develops a *SV-PMU microservice* (IEEE/IEC 60255-118-1:2018 performance – P-class), implemented via software in a generic hardware platform like an EDGE Server. The implementation was done using Docker containers [25] and microservices, following the instructions defined in the standards [8] [9] [10] [11].
- Two methods were implemented for the evaluation of the PMUs' behaviour. The first is a real-time evaluation using a Real-Time Automation Controller, and the second is an offline evaluation using a Python Script. The evaluation was conducted according to the limits defined in [8].

This work is part of the EPICS project (Edge Protection and Intelligent Control in Substations) [26]. This implementation enhances the number of microservices

provided by the EPICS platform, which final goal is to operate as a Centralized Protection and Control system in the Digital Substations, with the capability to feed with accurate measurements a WAMS or WAMPAC system associated with a Transmission or Distribution electrical system. Parts of this work were previously presented in [27] during IEEE AMPS 2024 congress and are extended in this document.

The new contributions compared with the IEEE AMPS 2024 congress include: The performance evaluation is done by implementing de *SV-PMU microservice* with a real-time patch to the Linux kernel. An additional *SV-PMU microservice* implementation has been done to obtain Synchrophasor measurements with lower latency. New tests, like modulation tests (Measurement Bandwidth) and latency measurements, are included. Additionally, the performance of the *SV-PMU microservice* is compared with that of a commercial PMU.

The paper is structured as follows. Section II presents a general description of the EPICS platform. Section III describes the implementation of the *SV-PMU microservice*. Section IV outlines the laboratory infrastructure used during this work. Section V details the tests executed and the evaluation criteria for the *SV-PMU microservice*. Section VI presents the test results. Finally, Section VII presents the conclusions.

II. EPICS PLATFORM DESCRIPTION

EPICS is a software-based CPC platform, designed to execute protection, control and automation algorithms in digital substations in a centralized way. EPICS separates hardware and software in protection and control systems and implements an architecture based on containerized microservices executed on generic hardware such as a conventional server. Then, EPICS platform is not built using vendor-specific software nor hardware. It is worth noting that EPICS is tested over a server Lenovo ThinkSystem SE350 with 16 Intel Xeon D-2183IT (16 cores) at 2.2 Ghz with 64 GB of memory. The server has an “Edge Computing” design with significant smaller dimensions than traditional servers giving enough flexibility for its installation in field. The operating system used in that server was Rocky Linux 9.0. In this work, the PREEMPT_RT patch [28] was applied to the Linux kernel in order to give to the kernel real-time capabilities such as priority inheritance, threaded interrupt handlers and high resolution timers. This patch minimizes the non-preemptible code in the kernel allowing to reduce the worst-case latencies. Additionally, the use of real-time programming techniques, real-time schedulers and system configuration [29] helped also to contain these latencies as it can be seen in the latency results of this work.

Currently, different developments have been implemented in the EPICS platform. For example, [30] explains the implementation related to an analog processing module based on IEC61850, [31] provides more details about the infrastructure of the EPICS platform, and [32] describes the implementation of a novel faulted phase selection algorithm for a distance protection.

> REPLACE THIS LINE WITH YOUR MANUSCRIPT ID NUMBER (DOUBLE-CLICK HERE TO EDIT) <

III. IMPLEMENTATION OF SV-PMU MICROSERVICE

Within the context of the EPICS project, the necessity arises to improve the capabilities of the EPICS platform, including a new feature able to provide PMU measurements using the voltage and current measurements supplied by the multiple SAMUs installed in the digital substations. The main goal for this work is to implement the PMU microservice, called the “SV-PMU microservice”, in the EPICS platform and evaluates its behaviour considering the performance requirements specified in the standards.

Multiple PMU algorithms exist in the literature, and their theoretical principles and performance are compared through simulations in [33]. However, the implementation of the SV-PMU microservice described and tested in this work is based on the transcription of the reference signal processing models, specifically P-class, as described in both IEEE C37.118.1-2011 Annex C [9] [10] and IEEE/IEC 60255-118-1:2018 Annex D [8]. These reference models describe the algorithms and filters used to obtain phasors from timestamped sampled signals. In that way, the Sampled Values fulfilling the time requirements of the IEC 61869-9 [34] standard, as the generated by a SAMU, are an example of those kind of sampled signals.

In particular, the Annexes describe the low pass filter for both P-class and M-class phasors, the quadrature oscillator used to calculate the complex value of the phasor for each single phase, the timestamp compensation for low pass filter group delay, and the estimation of frequency and ROCOF using the positive sequence phasor obtained by the symmetrical component transformation of the single phase phasors.

Two versions of the SV-PMU microservice were implemented during this work, the first one uses a two-cycle Finite Impulse Response (FIR) filter, and the second one uses a one-cycle FIR filter. The former follows the Reference signal processing model defined in the standard and latter tries to optimize the first one in order to give a synchrophasor value with lower latency.

Related with the timestamping of the computed phasors, the FRACSEC and SOC values are calculated by considering the SV *smpCnt* counter that is synchronized as stated in IEC 61869-9 (synchronized by PTP protocol in this work) and assured by the phase displacement limits for different accuracy classes described in IEC 61869-13[35]. In this way, the relative timestamp of a sample inside a second (FRACSEC in PMU protocol) is calculated by considering $FRACSEC = smpCnt \times sampling_period$. The seconds of the timestamp (SOC in the PMU protocol) of the synchrophasor is calculated using the absolute timestamping of the server system time and deducing the second which this *smpCnt* belongs. It should be noted that during this work the NTP in the local network was used as the method for system time synchronization (see section IV). It has to be remarked that the NTP client reported a maximum time error $< 300 \mu s$ and the offset $< 10 \mu s$ and then, the NTP time synchronization of the system is enough to identify the SOC of the synchrophasor.

A general diagram of the implementation of the SV-PMU microservice in the EPICS platform can be observed in Fig. 1.

The platform can manage and process multiple IEC 61850 Sampled Values (SV) frames published by the SAMUs installed in field using the *i61svs* microservice. The outputs of the *i61svs* microservice are available to be used by multiple protection and control microservices. For this implementation, the outputs of the *i61svs* microservice are used by the SV-PMU microservice to calculate and generate the PMU servers needed for each implementation.

The SV-PMU microservice implemented during this work is a versatile microservice because it could manage at the same time multiple sampled values frames existent in the field, calculates all synchrophasors and finally serve to multiple PMU clients depending on their needs. The SV-PMU microservice is composed of three layers. The first layer, called the PMU generator, uses the outputs of the *i61svs* microservice to calculate the synchrophasors of each sampled value frame. The resulting synchrophasors are stored and managed by an interprocess communication module called the PMU REAL-TIME DATA MANAGER (second layer), where all the resulting synchrophasor information are available to be accessed by the PMU servers module (third layer). The third layer is responsible for creating all the PMU servers needed by the specific application, and each server will be subscribed to by the PMU clients (typically Phasor Data Concentrators PDCs) that are external to the EPICS Platform. The SV-PMU microservice implemented during this work has a reporting rate of 50 frames per second (50 Hz).

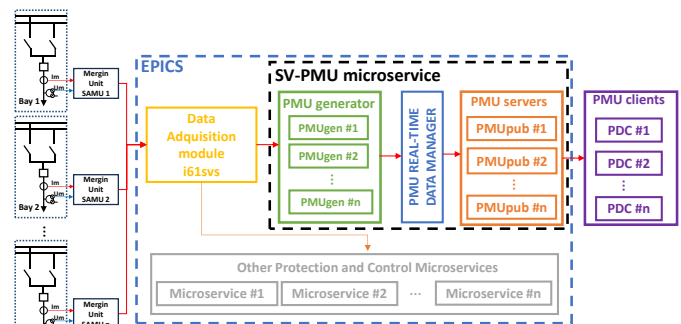


Fig. 1. General diagram of SV-PMU microservice in EPICS Platform.

IV. LABORATORY INFRASTRUCTURE

A general diagram of the laboratory testbed used in this work is presented in Fig. 2. As illustrated in the figure, the testbed primarily consists of the following components:

- A Real-Time digital simulator (RTDS): Generates any type of synthetic signals required for the evaluation of the “SV-PMU microservice”.
- A GTNETx2 SV module of the RTDS: Publishes IEC61850 SV stream (“RTDS IEC61850 SV”) at 4 kHz, equivalent to 80 samples per cycle in compliant with [17].
- A GTNETx2 PMU module of the RTDS: It operates as a PMU server (“Server PMU-RTDS”) and is capable of generating a synchrophasor frame in compliance with

> REPLACE THIS LINE WITH YOUR MANUSCRIPT ID NUMBER (DOUBLE-CLICK HERE TO EDIT) <

standards [9] [10]. The RTDS is time synchronized using PTP protocol. During this study, a P-class synchrophasor was used.

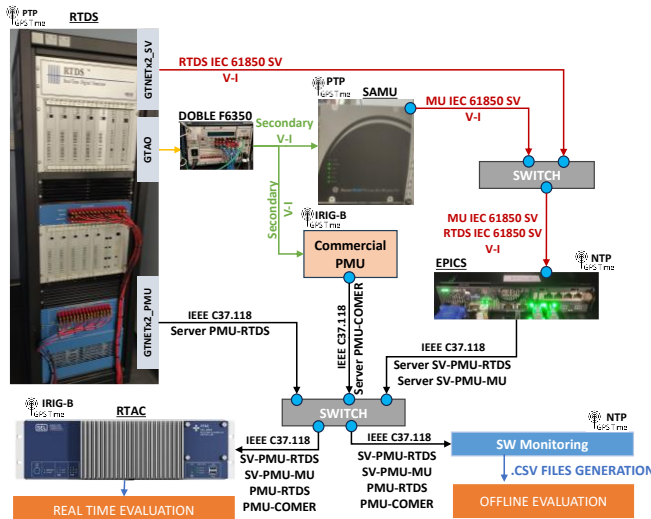


Fig. 2. General diagram of Laboratory testbed.

- **The GTA0 card of the RTDS:** Converts the current and voltage signals provided by the simulation into low-level analog signals (+/- 10 V) needed by power amplifier.
- **Power amplifier (Doble F6350):** It converts the low-level analog signals provided by GTA0 into suitable phase to ground secondary values ($63.5 V_{sec}$, $1A_{sec}$) to be connected to a conventional PMU and SAMU. Then, both devices will receive the same input signals during the evaluation process, ensuring that the errors and accuracy associated with GTA0 and the power amplifier affect both devices in the same way.
- **A commercial SAMU (“Reason MU320”):** Converts the secondary voltage and current values provided by the power amplifiers into IEC 61850 SV frames (“MU IEC61850 SV”) according to [17]. The sampling frequency of this equipment is 4000 SPS (80 s/cycle).
- **A commercial PMU (“PMU-COMER”):** Converts the secondary voltages and current values provided by the power amplifiers into P-class synchrophasor frames (“Server PMU-COMER”) according to [9] [10] [11].
- **EPICS platform:** The *SV-PMU microservice* and auxiliary services are implemented on the platform. The EPICS platform subscribes to both the “RTDS IEC61850 SV” and “MU IEC61850 SV” streams, and it is responsible for generating the PMU servers called “SV-PMU-RTDS” and “SV-PMU-MU”, using two instances of the *SV-PMU microservice*.
- **Real-Time Automation Controller (RTAC) SEL-3555:** [36]. This equipment is used during the real time validation stage of the *SV-PMU microservice*. It will manage the PMU information published by the EPICS platform (“SV-PMU-RTDS” and “SV-PMU-MU”) as well as the commercial PMU (“PMU-COMER”).
- **Synchrowave monitoring (SW)** [37]. This commercial software tool is used during the offline validation stage

of the *SV-PMU microservice*. It will manage the PMU information published by EPICS platform (“SV-PMU-RTDS” and “SV-PMU-MU”) as well as the commercial PMU (“PMU-COMER”).

The RTDS modules (GTNETx2_SV, GTNETx2_PMU and GTA0) use the same voltages and currents values generated by the real-time digital simulation as input signals, ensuring valid comparisons between PMUs (“PMU-COMER”, “SV-PMU-RTDS”, “PMU-RTDS” and “SV-PMU-MU”). Furthermore, all the devices are time-synchronized using a GPS Clock (SEL-2488). The time synchronization protocol used by each device during this work is specified in Fig. 2. The GPS clock has a peak time stamp accuracy of ± 100 ns for PTP and demodulated IRIG B protocols, and <100 μ s for NTP protocol. A PTP-compliant Ethernet switch (Hirshmann Greyhound) was used to distribute the PTP frames. Both the RTDS and the SAMU reported being time-synchronized (Clock Locked) with PTP, achieving a time quality accuracy of <1 μ s. The NTP protocol is used to synchronize the EPICS server, allowing the identification of the synchrophasor timestamp SOC, as explained in section III, and the frame timestamping during latency measurements testing, as explained in section V.

Finally, it is necessary to highlight that both the SAMU and the *PMU-COMER* have the same settings related to the voltage and current conversion ratios to ensure the correct calculation of the primary voltage and current values associated with the secondary values injected by the power amplifier.

V. TEST DESCRIPTION AND EVALUATION CRITERIA

This section includes a description of the tests carried out to check *SV-PMU microservice* operation (subsection A). Furthermore, the tolerances selected during tests are summarized in subsection B. A detailed description of the methodology used to check the *SV-PMU microservice* operation is described in subsection C. Finally, in subsection D is explained the latency performance evaluation method.

A. Tests description.

To assess the performance of the *SV-PMU microservice* implemented on EPICS platform, the outputs of the *SV-PMU-RTDS* and *SV-PMU-MU*, generated by the microservice, were evaluated. A series of steady-state, transient-state and latency tests were conducted to evaluate the operation of the *SV-PMU microservice*. These tests were selected from the IEEE/IEC 60255-118-1:20218 standard [8]. Following, the tests included during the study are listed:

a) Steady state tests.

Steady state tests have a duration of 10 minutes. Following, these tests are listed:

- **Signal frequency tests:** The operation is checked when the frequency of the voltage and current sources is 48, 50 and 52 Hz. Intermediate values of frequency were not considered during this work because the worst values of

> REPLACE THIS LINE WITH YOUR MANUSCRIPT ID NUMBER (DOUBLE-CLICK HERE TO EDIT) <

Total Vector Error (TVE), Frequency Error (FE) and Rate of change of Frequency Error (RFE) are expected in the tests associated with the frequency limits (48 Hz or 52 Hz), as demonstrated in [33].

- **Signal magnitude voltage tests:** The operation is monitored when the magnitude of the voltage sources is at 80 %, 100 % and 120 % of the rated voltage. During tests, a rated voltage of 230 kV phase-neutral is considered (63.5 V phase-neutral secondary). Intermediate values of voltages were not considered during this work because the worst values of TVE, FE and RFE are expected in the tests associated with the lower voltage limit (80 %).
- **Signal magnitude current tests:** The operation is evaluated when the magnitude of the current sources is at 10 %, 100 % and 200 % of the rated current. During tests, a rated current of 2 kA is considered (1 A secondary). Intermediate values of currents were not considered during this work because the worst values of TVE, FE and RFE are expected in the tests associated with the lower current limit (10 %).
- **Harmonic distortion tests:** The operation is examined when there are harmonics in the voltage, as specified in [8].

b) *Transient state tests.*

- **Measurement Bandwidth:** The test involves applying sinusoidal modulation to both the amplitude and phase angle of the three-phase input signals (voltage and current sources). The amplitude modulation and phase angle factor cannot be applied simultaneously, and each is limited to a maximum value of 0.1. Additionally, a modulation frequency in the range of 0.1 to 2 Hz is applied during the tests.
- **Frequency ramp tests:** The operation is tested when the frequency of the voltage and current sources vary periodically from 48 to 52 Hz (triangular behaviour), with a ramp rate of ± 1 Hz/s. This test lasts for 10 minutes.
- **Step Change in Magnitude:** These tests involve generating a voltage and current step of 1.1 p.u. and 0.9 p.u.
- **Step Change in Angle:** $+10^\circ$ and -10° steps in the current angle.

c) *Latency tests.*

During these tests, the latencies of the PMUs are measured. The PMU latency is defined as the time difference between the synchrophasor timestamp and the time when this synchrophasor leaves the PMU communication port [8].

The latency must be evaluated for at least 20 minutes, during this work the latency was evaluated for 30 minutes following the recommendation of the standard [8].

B. *Evaluation criteria.*

The performance of the PMU is evaluated, as outlined in [8], by calculating the Total Vector Error (TVE), Frequency Error (FE) and Rate of change of Frequency Error (RFE). The tolerances used to assess the behaviour of the *SV-PMU microservice* and commercial PMU outputs are provided in

TABLE I.

The analog to digital conversion process of the voltage and current measurement, executed by an instrument transformer or SAMU, have intrinsic errors that are considered in the threshold limits presented in TABLE I. However, when this digitalization process does not exist, the thresholds limits used for the evaluation of the PMU algorithm must be reduced according to the standard [8]. This specific case applies to the performance evaluation of the *SV-PMU-RTDS* and the threshold limits are detailed in TABLE II. At rated frequency, the standard [8] indicates that the conversion algorithms are very precise and contribute almost no error, reducing the limit of TVE up to 0.01%. For off rated frequency tests, the reduced limit of the TVE is 0.5%. Related with the Frequency and ROCOF accuracy under steady-state conditions, the limits are reduced by a factor of 2, i.e. FE= 0.0025 Hz and RFE=0.2 Hz/s. In transient state conditions, the thresholds limits are the same than presented in TABLE I.

TABLE I.
CONTROL VARIABLES THRESHOLDS TO CHECK SV-PMU
MICROSERVICE OUTPUTS

Control Variables	Steady State Tolerances	Transient State Tolerances
Max TVE (%)	1	1
Max FE (Hz)	0.005	0.01
Max RFE (Hz/s)	0.4	0.4

TABLE II.
CONTROL VARIABLES THRESHOLDS TO CHECK SV-PMU-RTDS
OUTPUTS

Control Variables	Steady State Tolerances	Transient State Tolerances
Max TVE (%)	$\frac{0.01 \text{ at rated frequency}}{0.5 \text{ off rated frequency}}$	1
Max FE (Hz)	0.0025	0.01
Max RFE (Hz/s)	0.2	0.4

For the frequency ramp tests, the exclusion intervals defined in [8] were considered. The TVE, FE and RFE values were ignored when the frequency exceeded 51.92 Hz or was below 48.04 Hz. The exclusion intervals are used to disregard transitory transitions when the frequency slope changes during the test.

For the Step tests, the standard [8] specifies a maximum overshoot/undershoot equal to 5 % of the step, with a response time for TVE of less than 60 ms (3 reporting intervals), a response time for frequency of less than 0.09 s, and a response time for ROCOF of less than 0.12 s.

For the measurement bandwidth test (modulation tests), the standard [8] specifies higher thresholds than those described in Table I. In this scenario, the new thresholds are TVE=3 %, FE= 0.06 Hz and RFE=2.3 Hz/s for a reporting rate equal to 50 Hz.

For latency evaluation, the standard [8] specifies that the maximum allowed latency for PMU is 42 ms.

The laboratory testbed described in Section IV is used to evaluate the operation of the *SV-PMU microservice*. Additionally, the testbed is utilized to obtain measurements from a commercial PMU, which are used for comparison with

> REPLACE THIS LINE WITH YOUR MANUSCRIPT ID NUMBER (DOUBLE-CLICK HERE TO EDIT) <

microservice operation.

C. Evaluation methods for TVE, FE and RFE

As said before in section IV, The RTDS modules (GTNETx2_SV, GTNETx2_PMU and GTA0) use the same voltages and currents values generated by the real-time digital simulation as input signals, ensuring valid comparisons between PMUs “*PMU-COMER*”, “*SV-PMU-RTDS*”, “*PMU-RTDS*” and “*SV-PMU-MU*”.

The signal provided by *PMU-RTDS* server is used as reference during the evaluation process, for the calculation of the TVE, FE and RFE. The standard [8] specifies that a traceable synchronized signal generator shall be used to verify the performance. In absence of that generator, the *PMU-RTDS* is used as reference. In [38] extensive tests were done to the GTNETx2_PMU module obtaining good results. In [39] and [40] is expressed that the GTNETx2_PMU module has a TVE<0.01 % at their test facilities which trace back to metrological authority. This value enables the possibility to use the *PMU-RTDS* as a valid reference for PMU evaluations in the 1 % TVE limit.

Two evaluation methods have been used during this study. The first method focuses on assessing the real-time performance of the *SV-PMU microservice*, while the second method involves an offline evaluation. Following, a detailed description of these methods is carried out.

- a) Real-time evaluation method: The RTAC SEL-3555, described in section IV, is employed to carry out this task. The evaluation criteria (TVE, FE and RFE), previously defined, are implemented within the RTAC using the IEC 61131-3 programming language [41], [42], [43]. The evaluation process involves continuously monitoring and comparing the outputs of the *SV-PMU microservices* (*SV-PMU-RTDS* and *SV-PMU-MU*), as well as those of the commercial PMU (*PMU-COMER*), against the reference values provided by “*PMU-RTDS*”. If any of the monitored values exceed the tolerance limits defined in [8], a COMTRADE file is generated for post-mortem analysis.
- b) Offline mode evaluation method: This method is performed in offline mode using a Python script to process the .CSV files generated by the Synchronwave Monitoring software (SWM) [37]. The script calculates the TVE, RFE and FE of the *SV-PMU microservice* outputs (*SV-PMU-RTDS* and *SV-PMU-MU*) as well as evaluates the performance of the commercial PMU (*PMU-COMER*), using the values from “*PMU-RTDS*” as a reference. The script outputs the maximum, average, standard deviation and tolerance evaluation for the TVE, RFE and FE.

D. Evaluation methods for latency

Two different kinds of measurements have been designed to characterize the PMUs latency during this work: First, in the case of *SV-PMU microservice*, the time is measured between the timestamp of the measured synchrophasor and the

time when it is sent by the EPICS platform. Second, in the case of *PMU-COMER*, the time is measured between the timestamp of the *PMU-COMER* synchrophasor and the time when it is received by the EPICS platform, giving an upper bound latency scenario in this case. The evaluation of the time of communication is obtained using tcpdump command and synchronizing the system with the GPS Clock via NTP. In this work the offset and max error of the NTP synchronization has been also monitored as can be seen in the results (section VI). The latency data was stored for 30 minutes. During this tests it is verified that the measured latency is lower than the required by the standard (<42 ms) [8].

VI. TEST RESULTS

This section summarizes the most representative results obtained from tests described in Section V. It includes the performance of the control variables (TVE, FE, RFE) for each testing scenario. Subsection A presents the performance of the *SV-PMU microservice* when the EPICS input signal comes from RTDS (*SV-PMU-RTDS*). The performance of the *SV-PMU microservice* when the input signal comes from a SAMU using a two-cycle FIR (*SV-PMU-MU “two-cycle FIR”*) and one-cycle FIR filter (*SV-PMU-MU “one-cycle FIR”*) is presented in Subsection B and Subsection C, respectively. Subsection D compares the performance between the commercial PMU (*PMU-COMER*) and the *SV-PMU-MU “one-cycle FIR”*. The evaluation of the PMUs’ performance is based on the criteria defined in Section V.

A. *SV-PMU-RTDS Results*

a) Steady state test results.

TABLE III presents the maximum values of TVE, FE and RFE obtained during steady-state tests. Based on these results, it is concluded that in all study cases, the TVE, FE and RFE values fall within the defined limits. The maximum TVE value was obtained during the frequency test at 52 Hz, reaching 0.206 % (Mean value = 0.148 %, Standard deviation “ σ ” = 0.0452 %).

TABLE III.
STEADY STATE TEST RESULTS, SV-PMU-RTDS

Type test	Max TVE (%)	Max FE (Hz)	Max RFE (Hz/s)	Inside limits
Magnitude Voltage	8.73E-05	0	2.64E-07	☑
Magnitude Current	0.00045	0	2.12E-07	☑
Harmonic distortion	0.02047	0	2.29E-07	☑
Frequency	0.206	0	2.86E-06	☑

b) Transient state results

These tests are divided into Frequency ramp test and Step Change in magnitude and angle. During the Frequency Ramp test, the highest recorded TVE, FE and RFE values were 0.188 %, 0.00135 Hz and 0.0086 Hz/s respectively. Those values are inside the limits defined by [8].

On the other hand, test results from Step Change in magnitude and voltage are detailed TABLE IV. The obtained results during tests are inside the limits defined by [8].

As can be seen in the test results of the *SV-PMU-RTDS*, the

> REPLACE THIS LINE WITH YOUR MANUSCRIPT ID NUMBER (DOUBLE-CLICK HERE TO EDIT) <

obtained values of TVE, FE and RFE are very low, indicating that the performance of *SV-PMU-RTDS* is very similar to the reference values (“*PMU-RTDS*”). This suggests that the implementation of the *SV-PMU microservice* in the EPICS platform is correct. However, this scenario is highly idealized and unlikely to occur in the real world because the *SV-PMU-RTDS* is obtaining the measurements directly from RTDS, without any perturbation or real measurement element like a SAMU.

TABLE IV.
STEP CHANGE IN MAGNITUDE, *SV-PMU-RTDS*

Test	Step Magnitude	Response time (ms)	Max Overshoot/undershoot (%)
Step in Voltage	1 p.u. to 1.1 p.u.	< 60 ms	0 %
Magnitude	1 p.u. to 0.9 p.u.	< 60 ms	0 %
Step in Current	1 p.u. to 1.1 p.u.	< 60 ms	0 %
Magnitude	1 p.u. to 0.9 p.u.	< 60 ms	0 %
Step in Angle	+10°	< 60 ms	0 %
Step in Angle	-10°	< 60 ms	0 %

To extrapolate the use of the *SV-PMU microservice* to the real world, a SAMU was used to measure the secondary voltages and currents generated by the RTDS using the power amplifier (Doble F6350). This scenario is more applicable, and the results can be compared with a commercial PMU.

The next subsection presents the tests results of the *SV-PMU microservice* using a two-cycle FIR filter (*SV-PMU-MU “Two-cycle FIR”*) and the sampled values provided by the SAMU.

B. *SV-PMU-MU “Two-cycle FIR” Results*

The test results of the *SV-PMU-MU “Two-cycle FIR”* implementation are shown below.

a) Steady state test results.

TABLE V presents the test results obtained during steady-state tests, when a two-cycle FIR filter is implemented. Based on these results, it can be concluded that in the cases of magnitude voltage, harmonic distortion and frequency tests, the values obtained for TVE, FE and RFE fall within the defined limits. The maximum TVE value was obtained during the frequency test at 48 Hz, reaching 0.691 % (Mean value = 0.301 %, Standard deviation “ σ ” = 0.0868 %).

TABLE V.
STEADY STATE TEST RESULTS, *SV-PMU-MU “Two-cycle FIR”*

Type test	Max TVE (%)	Max FE (Hz)	Max RFE (Hz/s)	Inside limits
Magnitude Voltage	0.588	0.000473	0.037	☑
Magnitude Current	7.12	0.001003	0.071	☑
Harmonic distortion	0.554	0.00134	0.1017	☑
Frequency	0.691	0.00048	0.038	☑

In the case of magnitude current tests, it is observed that the maximum TVE value exceeds the preset limit. This happens in the test with 10 % of rated current where the current magnitude is lower and any deviation in current magnitude will be traduced in big deviations in the TVE of the currents. In the tests with 100 % and 200 % of rated currents, the TVE is within the limits defined by [8]. For additional

information, in TABLE VI is represented the TVE values (Maximum, mean and σ) of the current signals obtained during the Magnitude Current tests.

As an example, a summary of the TVE results obtained by the *SV-PMU-MU “Two-cycle FIR”* in the frequency tests can be observed in TABLE VII. The table shows the performance of “Max TVE”, “Mean TVE” and “TVE σ ” depending on the frequency of the test and the type of signal analyzed (current or voltage). As can be observed, the lower values of TVE are obtained during voltage synchrophasors analysis (Max TVE of voltage=0.410 % at 48 Hz). Furthermore, the maximum TVE value occurs during the evaluation of the current synchrophasors at 48 Hz.

TABLE VI.
TVE VALUES, MAGNITUDE CURRENT TEST
SV-PMU-MU “Two-cycle FIR”

Current magnitude	Signal	Max TVE (%)	Mean TVE (%)	TVE σ (%)	Inside limits
10 %	Ia	5.285	4.418	0.1984	☒
	Ib	7.124	6.230	0.2329	☒
	Ic	4.056	3.278	0.2277	☒
100 %	Ia	0.502	0.203	0.0753	☑
	Ib	0.462	0.143	0.0664	☑
	Ic	0.525	0.216	0.0860	☑
200 %	Ia	0.548	0.504	0.0098	☑
	Ib	0.288	0.248	0.0107	☑
	Ic	0.636	0.586	0.0122	☑

TABLE VII.
TVE VALUES, FREQUENCY TEST
SV-PMU-MU “Two-cycle FIR”

Frequency	Signal	Max TVE (%)	Mean TVE (%)	TVE σ (%)	Inside limits
48 Hz	Ia	0.691	0.301	0.0868	☑
	Ib	0.658	0.264	0.1065	☑
	Ic	0.687	0.312	0.0961	☑
	Va	0.384	0.225	0.0399	☑
	Vb	0.410	0.263	0.0394	☑
	Vc	0.387	0.232	0.0398	☑
50 Hz	Ia	0.502	0.203	0.0753	☑
	Ib	0.462	0.143	0.0664	☑
	Ic	0.525	0.216	0.0860	☑
	Va	0.151	0.051	0.0162	☑
	Vb	0.191	0.105	0.0122	☑
	Vc	0.158	0.059	0.0161	☑
52 Hz	Ia	0.513	0.184	0.0806	☑
	Ib	0.507	0.173	0.0852	☑
	Ic	0.550	0.196	0.0869	☑
	Va	0.221	0.133	0.0466	☑
	Vb	0.227	0.143	0.0460	☑
	Vc	0.214	0.125	0.0462	☑

b) Transient state results.

These tests are divided into Frequency ramp test, modulation tests in magnitude and phase angle, and Step Change in magnitudes and angle.

TABLE VIII includes the Frequency ramp and modulation tests results for the *SV-PMU-MU (two-cycle FIR)*. The test results from Step Changes are detailed in TABLE IX. All the results are inside the limits defined by [8].

> REPLACE THIS LINE WITH YOUR MANUSCRIPT ID NUMBER (DOUBLE-CLICK HERE TO EDIT) <

TABLE VIII.
FREQUENCY RAMP AND MODULATION TESTS,
SV-PMU-MU "Two-cycle FIR"

Test	Max. TVE (%)	Max. FE (Hz)	Max. RFE (Hz/s)	Inside limits
Frequency ramp	0.638	0.001732	0.0351	✓
Modulation in amplitude	0.644	0.00064	0.035	✓
Modulation in phase angle	0.514	0.01073	0.734	✓

TABLE IX.
STEP CHANGE IN MAGNITUDE, *SV-PMU-MU "Two-cycle FIR"*

Test	Step Magnitude	Response time (ms)	Max (%) Overshoot/undershoot
Step in Voltage	1 p.u. to 1.1 p.u.	< 60 ms	0.93 %
Magnitude	1 p.u. to 0.9 p.u.	< 60 ms	0.69 %
Step in Current	1 p.u. to 1.1 p.u.	< 60 ms	2.01 %
Magnitude	1 p.u. to 0.9 p.u.	< 60 ms	3.53 %
Step in Angle	+10°	< 60 ms	0.58 %
Step in Angle	-10°	< 60 ms	0.57 %

c) Latency measurement.

The theoretical expected latency of the *SV-PMU microservice* using a two-cycle FIR filter is 40 ms as it is explained in [8].

The measured latencies of *SV-PMU microservice* using a two-cycle FIR filter can be observed in Fig. 3 (Blue color). The average value and the standard deviation obtained during the evaluation were 40.88 ms and 0.00248 ms, respectively. The measured worst case was below 40.97 ms. It is important to note that those latency values are affected by the NTP error. The NTP maximum error reported by the NTP server was always below 300 μs during these tests. Taking that into account, the measured latency is lower than required by the standard (<42 ms) [8].

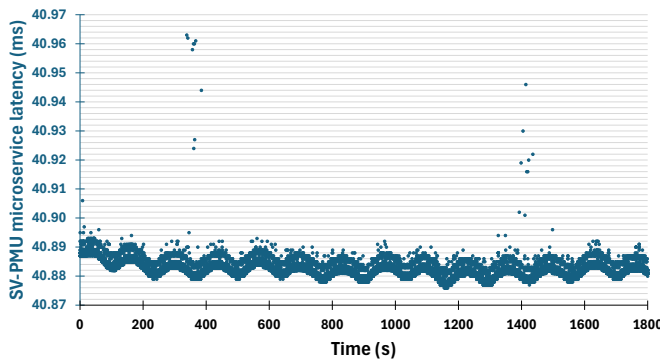


Fig. 3. *SV-PMU-MU "Two-cycle FIR"*, Latency measurements.

Observing the latency associated with the implementation of the *SV-PMU-MU "Two-cycle FIR"*, a new version of the *SV-PMU microservice* using one-cycle FIR filter (*SV-PMU-MU "One-cycle FIR"*) was implemented to achieve a lower latency and its performance can be observed in the following section.

C. *SV-PMU-MU "One-cycle FIR" Results*

In this section, the test results of the *SV-PMU-MU "One-cycle FIR"* implementation are presented.

a) Steady state test results.

TABLE X presents the test results obtained during steady-state tests, when a one-cycle FIR filter is implemented. Based on these results, it can be concluded that in the cases of magnitude voltage, harmonic distortion and frequency tests, the values obtained for TVE, FE and RFE fall within the defined limits. The maximum TVE value was obtained during the harmonic distortion test, reaching 0.823 % (Mean value = 0.792 %, Standard deviation “σ” = 0.0085 %).

In the case of magnitude current tests, it is observed that the maximum TVE value exceeds the preset limit. This happens, as previously mentioned in the *SV-PMU-MU "Two-cycle FIR"* results, in the test with 10 % of the rated current. In the tests with 100 % and 200 % of rated currents, the TVE is within the limits defined by [8].

TABLE X.
STEADY STATE TEST RESULTS, *SV-PMU-MU "One-cycle FIR"*

Type test	Max TVE (%)	Max FE (Hz)	Max RFE (Hz/s)	Inside limits
Magnitude Voltage	0.546	0.0001003	0.069	✓
Magnitude Current	1.52	0.001003	0.069	✗
Harmonic distortion	0.823	0.0033	0.234	✓
Frequency	0.781	0.00126	0.071	✓

As an example, a summary of the TVE results obtained by the *SV-PMU-MU "One-cycle FIR"* in the frequency tests can be observed in TABLE XI. It shows that the TVE of voltages and currents are inside the TVE limit. As can be observed in the table, the lower values of TVE are obtained during voltage synchrophasors analysis (Max TVE of voltage=0.620 % at 48 Hz). Furthermore, the maximum TVE value (0.781%) occurred during the evaluation of the current synchrophasors at 52 Hz.

TABLE XI.
TVE VALUES, FREQUENCY TEST
SV-PMU-MU "One-cycle FIR"

Frequency	Signal	Max TVE (%)	Mean TVE (%)	TVE σ (%)	Inside limits
48 Hz	Ia	0.671	0.504	0.0745	✓
	Ib	0.720	0.525	0.0862	✓
	Ic	0.632	0.469	0.0713	✓
	Va	0.496	0.386	0.0670	✓
	Vb	0.620	0.465	0.0765	✓
	Vc	0.554	0.386	0.0805	✓
50 Hz	Ia	0.459	0.405	0.0144	✓
	Ib	0.466	0.382	0.0221	✓
	Ic	0.479	0.399	0.0203	✓
	Va	0.404	0.387	0.0056	✓
	Vb	0.534	0.512	0.0061	✓
	Vc	0.348	0.326	0.0060	✓
52 Hz	Ia	0.711	0.513	0.0805	✓
	Ib	0.781	0.536	0.0959	✓
	Ic	0.658	0.481	0.0756	✓
	Va	0.483	0.367	0.0749	✓
	Vb	0.553	0.433	0.0814	✓
	Vc	0.489	0.362	0.0838	✓

Finally, it should be noticed that the maximum TVE values obtained from both the *SV-PMU-MU "One-cycle FIR"* and *SV-PMU-MU "Two-cycle FIR"* implementations, fulfil the standard requirements. Furthermore, in voltage synchrophasor analysis, the implementation of *SV-PMU-MU*

> REPLACE THIS LINE WITH YOUR MANUSCRIPT ID NUMBER (DOUBLE-CLICK HERE TO EDIT) <

“One-cycle FIR” shows an increment of the “Max TVE”, compared to the two-cycle FIR implementation (see TABLE VII).

b) *Transient state results.*

TABLE XII includes the frequency ramp and modulation tests results for the *SV-PMU-MU* “One-cycle FIR”. The test results from Step Changes are detailed in TABLE XIII. All the results are inside the limits defined by [8].

TABLE XII.
FREQUENCY RAMP AND MODULATION TESTS,
SV-PMU-MU “One-cycle FIR”

Test	Max. TVE (%)	Max. FE (Hz)	Max. RFE (Hz/s)	Inside limits
Frequency ramp	0.746	0.00248	0.072	☑
Modulation in amplitude	0.635	0.00105	0.065	☑
Modulation in phase angle	0.496	0.0245	0.762	☑

TABLE XIII.
STEP CHANGE IN MAGNITUDE, *SV-PMU-MU* “One-cycle FIR”

Test	Step Magnitude	Response time (ms)	Max (%) Overshoot/undershoot
Step in Voltage	1 p.u. to 1.1 p.u.	< 60 ms	1.52 %
	1 p.u. to 0.9 p.u.	< 60 ms	1.55 %
Step in Current	1 p.u. to 1.1 p.u.	< 60 ms	1.10 %
	1 p.u. to 0.9 p.u.	< 60 ms	1.13 %
Step in Angle	+10°	< 60 ms	0.05 %
Step in Angle	-10°	< 60 ms	-0.09 %

c) *Latency measurement.*

The theoretical expected latency of the *SV-PMU microservice* using a one-cycle FIR filter is 30 ms.

The measured latencies of *SV-PMU microservice* using a one-cycle FIR filter can be observed in Fig. 4 (Blue color). The average value and the standard deviation obtained during the evaluation were 30.86 ms and 0.00417 ms, respectively. The worst case measured was below 30.93 ms. The measured latency is lower than required by the standard (<42 ms) [8].

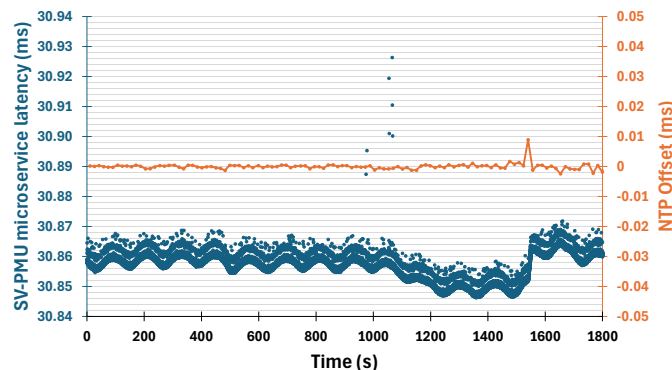


Fig. 4. *SV-PMU-MU* (one-cycle FIR), Latency measurements.

In Fig. 4 can be observed also the NTP Offset (Orange Color) reported by the data acquisition server. Near the second 1600 it is observed a correction of NTP time in the data acquisition server. That NTP correction had an evident effect on the latency measurement. Anyway, this graph is enough to assess that the latency of *SV-PMU microservice* using a one-

cycle FIR filter is below the limit stated in the standard. Furthermore, it should be noticed that the latency values measured using one cycle FIR implementation are improved compared to the latency values associated to *SV-PMU-MU* “Two-cycle FIR” implementation. For future works, the PTP time synchronization protocol may be used during latency measurement tests due to its better performance compared with NTP.

D. *Comparison between SV-PMU-MU and PMU-COMER.*

In this section, the behaviour of the *SV-PMU-MU* “One-cycle FIR” is compared with that obtained by the *PMU-COMER*. The comparison is done in terms of latency, steady-state and transient state performance. The *SV-PMU-MU* “One-cycle FIR” was selected for this comparison because it achieved good results in all tests and has the lowest latency compared to the *SV-PMU-MU* “Two-cycle FIR” implementation. It is necessary to highlight that the details of the synchrophasor calculation algorithms implemented by the manufacturer of the *PMU-COMER* are not known by the authors. However, its performance is compared with that obtained by the *SV-PMU-MU microservice* using a one-cycle FIR filter under the same testing scenarios and testing signals.

a) *Steady state comparison.*

TABLE XIV and TABLE XV present the TVE, FE and RFE values obtained during the frequency and the voltage magnitude tests, respectively. From test results can be concluded that the *SV-PMU-MU* performs better in terms of TVE and RFE compared to the *PMU-COMER*, but in terms of FE, it performs a little bit worse. However, both fulfil the standard requirements.

TABLE XIV.
TVE, FE AND RFE VALUES, FREQUENCY TEST
SV-PMU-MU “One-cycle FIR” and *PMU-COMER*

PMU	Value	Max	Mean	σ	Inside limits
<i>SV-PMU-MU</i>	TVE (%)	0.781	0.5358	0.0958	☑
	FE (Hz)	0.00126	0.000295	0.000206	☑
	RFE (Hz/s)	0.071	0.015103	0.011874	☑
<i>PMU-COMER</i>	TVE (%)	0.982	0.72	0.02369	☑
	FE (Hz)	0.00088	0.000301	0.00016	☑
	RFE (Hz/s)	0.102	0.036028	0.01951	☑

TABLE XV.
TVE, FE AND RFE VALUES, VOLTAGE MAGNITUDE TEST
SV-PMU-MU “One-cycle FIR” and *PMU-COMER*

PMU	Value	Max	Mean	σ	Inside limits
<i>SV-PMU-MU</i>	TVE (%)	0.546	0.52155	0.00638	☑
	FE (Hz)	0.001003	0.000201	0.000155	☑
	RFE (Hz/s)	0.069	0.014339	0.011474	☑
<i>PMU-COMER</i>	TVE (%)	0.674	0.60104	0.01838	☑
	FE (Hz)	0.00085	0.000304	0.000165	☑
	RFE (Hz/s)	0.09559	0.035741	0.019148	☑

TABLE XVI presents the TVE values obtained by the *SV-PMU-MU* and the *PMU-COMER* during the steady state current magnitude tests, under the scenario of 10% rated current. It is necessary to highlight that the maximum values

> REPLACE THIS LINE WITH YOUR MANUSCRIPT ID NUMBER (DOUBLE-CLICK HERE TO EDIT) <

of TVE were obtained by both PMUs in the current signals, reaching values around to the threshold limit. Furthermore, all the TVE values related with 100 % and 200% current magnitude tests fulfil the standard requirements.

Regarding the harmonic test behaviour, TABLE XVII summarizes the TVE, FE and RFE performance of the *SV-PMU-MU* “One-cycle FIR” and the *PMU-COMER* obtained during the test. From test results, it is concluded *PMU-COMER* performs better than the *SV-PMU-MU*, Nevertheless, the obtained value of TVE, FE and RFE in both PMUs are well below the limit required by the standard.

TABLE XVI.
TVE VALUES, MAGNITUDE CURRENT TEST: 10%
SV-PMU-MU “One-cycle FIR” and *PMU-COMER*

Current magnitude	Signal	Max TVE (%)	Mean TVE (%)	TVE σ (%)	Inside limits
<i>SV-PMU-MU</i>	Ia	1.126	0.347	0.1664	<input type="checkbox"/>
	Ib	1.518	0.628	0.2391	<input type="checkbox"/>
	Ic	0.864	0.247	0.1262	<input checked="" type="checkbox"/>
	Va	0.409	0.389	0.0056	<input checked="" type="checkbox"/>
	Vb	0.535	0.511	0.0061	<input checked="" type="checkbox"/>
<i>PMU-COMER</i>	Vc	0.350	0.328	0.0059	<input checked="" type="checkbox"/>
	Ia	0.973	0.395	0.1487	<input checked="" type="checkbox"/>
	Ib	0.899	0.305	0.1406	<input checked="" type="checkbox"/>
	Ic	0.778	0.250	0.1281	<input checked="" type="checkbox"/>
	Va	0.509	0.503	0.0017	<input checked="" type="checkbox"/>
<i>PMU-COMER</i>	Vb	0.545	0.539	0.0016	<input checked="" type="checkbox"/>
	Vc	0.506	0.499	0.0017	<input checked="" type="checkbox"/>

TABLE XVII.
TVE, FE AND RFE VALUES, HARMONIC TEST
SV-PMU-MU “One-cycle FIR” and *PMU-COMER*

PMU	Value	Max	Mean	σ	Inside limits
<i>SV-PMU-MU</i>	TVE (%)	0.823	0.792	0.0085	<input checked="" type="checkbox"/>
	FE (Hz)	0.003300	0.000722	0.000530	<input checked="" type="checkbox"/>
	RFE (Hz/s)	0.23384	0.05233	0.03983	<input checked="" type="checkbox"/>
<i>PMU-COMER</i>	TVE (%)	0.538	0.533	0.0016	<input checked="" type="checkbox"/>
	FE (Hz)	0.001026	0.000317	0.0001869	<input checked="" type="checkbox"/>
	RFE (Hz/s)	0.1286	0.0375	0.0223	<input checked="" type="checkbox"/>

b) Transient state comparison

Regarding the comparison of behaviour in the frequency ramp test, amplitude modulation tests and phase angle modulation tests, similar behaviour was observed between the *SV-PMU-MU* “One-cycle FIR” and the *PMU-COMER*. An example of the observed behaviour can be seen in Fig. 5, Fig. 6, Fig. 7 and Fig. 8. Those figures are related to the frequency ramp tests.

Fig. 5 includes a histogram of the TVE of the phase A current evaluated for both the *SV-PMU-MU* (orange) and the *PMU-COMER* (blue). It can be observed that the TVE band in both cases are very similar. The mean value and standard deviation of the histograms can be observed in the figure.

Fig. 6 includes a histogram of the TVE of the phase A voltage evaluated for both the *SV-PMU-MU* (orange) and the *PMU-COMER* (blue). In this case, it can be observed that the TVE band is different in both cases, with better results obtained by the *SV-PMU-MU*. Nevertheless, both PMUs meet the standard requirement. The mean value and standard deviation of the histograms can be observed in the figure.

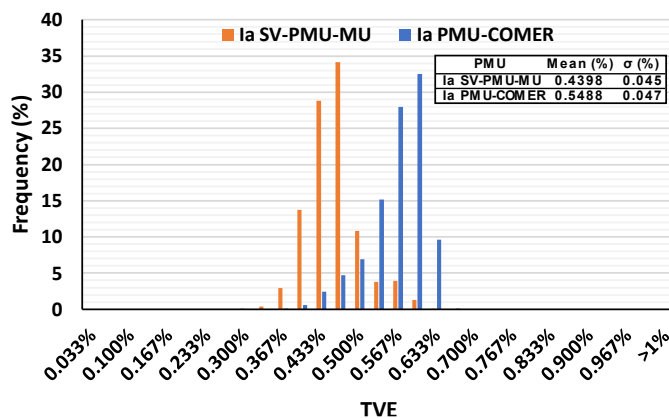


Fig. 5. Comparison, Frequency ramp test, TVE, Ia.

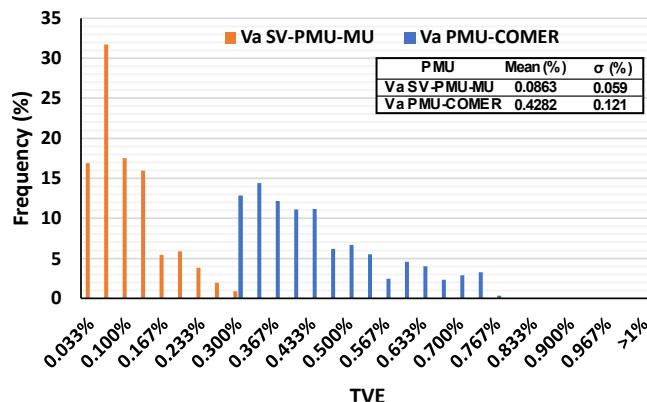


Fig. 6. Comparison, Frequency ramp test, TVE, Va.

Fig. 7 includes a histogram of the resulting FEs evaluated for both the *SV-PMU-MU* (orange) and the *PMU-COMER* (blue). It can be observed that the FE band in both cases is very similar. The mean value and standard deviation of the histograms can be observed in the figure.

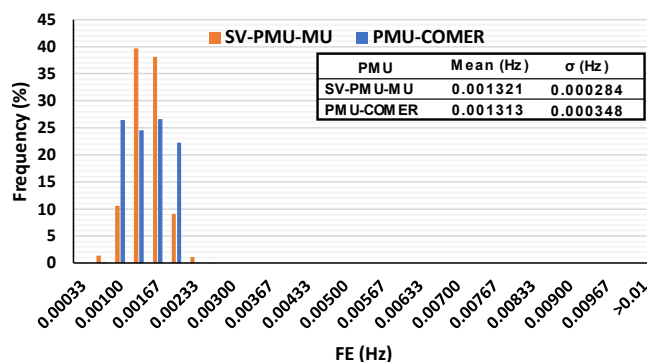


Fig. 7. Comparison, Frequency ramp test, FE.

Fig. 8 includes a histogram of the resulting RFEs evaluated for both the *SV-PMU-MU* (orange) and the *PMU-COMER* (blue). It can be observed that the RFE band in both cases is very similar. The mean value and standard deviation of the histograms can be observed in the figure.

Regarding the comparison of behaviour in amplitude and phase modulation test (See TABLE XVIII and TABLE XIX), it is concluded that the TVE and RFE of the *SV-PMU-MU* performs better than *PMU-COMER*. Nevertheless, the obtained value of TVE, FE and RFE in both PMUs are below the limit required by the standard.

> REPLACE THIS LINE WITH YOUR MANUSCRIPT ID NUMBER (DOUBLE-CLICK HERE TO EDIT) <

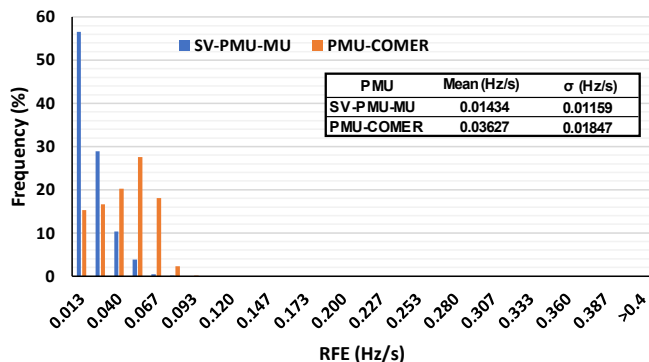


Fig. 8. Comparison, Frequency ramp test, RFE.

TABLE XVIII.

TVE, FE AND RFE VALUES, AMPLITUDE MODULATION TEST
SV-PMU-MU “One-cycle FIR” and PMU-COMER

PMU	Value	Max	Mean	σ	Inside limits
SV-PMU-MU	TVE (%)	0.635	0.383314	0.08436	✓
	FE (Hz)	0.00105	0.000216	0.000169	✓
	RFE (Hz/s)	0.065	0.014404	0.011533	✓
PMU-COMER	TVE (%)	0.828	0.608702	0.065941	✓
	FE (Hz)	0.000862	0.000301	0.000164	✓
	RFE (Hz/s)	0.092825	0.035182	0.018475	✓

TABLE XIX.

TVE, FE AND RFE VALUES, PHASE MODULATION TEST
SV-PMU-MU “One-cycle FIR” and PMU-COMER

PMU	Value	Max	Mean	σ	Inside limits
SV-PMU-MU	TVE (%)	0.495987	0.409137	0.016571	✓
	FE (Hz)	0.024497	0.001625	0.001899	✓
	RFE (Hz/s)	0.761985	0.124866	0.153737	✓
PMU-COMER	TVE (%)	0.7252	0.593841	0.038319	✓
	FE (Hz)	0.012211	0.001872	0.002194	✓
	RFE (Hz/s)	1.38212	0.129427	0.163558	✓

c) Latency measurement comparison.

In terms of latency measurements of the PMU-COMER, an upper bound latency was measured: a mean value of 28.54 ms with a standard deviation of 0.127 ms. This latency is like that obtained by the SV-PMU-MU “One-cycle FIR”: a mean value of 30.86 ms with a standard deviation of 0.00417 ms. The measured latency of the PMU-COMER is less than 30ms, which indicates that the PMU algorithm it uses is different from the one implemented by SV-PMU-MU “One-cycle FIR”.

It has to be noted that the values of latency of PMU-COMER and SV-PMU-MU cannot be precisely compared. On one hand, the timestamp for the PMU-COMER accounts also the trip time of the frame given the fact that it is measured when the frame arrives to the EPICS server, whereas SV-PMU-MU latency is measured when the frame reaches the network interface (NIC driver) during sending process. Additionally, the PMU-COMER time window and algorithm are unknown making it difficult to account the latency inherent to the time window. For the same reason it is also difficult to determine latency coming from processing and communications. In any case, the latency data measured here show their trend, considering the aforementioned limitations.

VII. CONCLUSIONS

During this work a SV-PMU microservice (Performance – P class) was successfully developed and implemented via software in a generic hardware platform like an EDGE Server, called EPICS Platform. The implementation was done using Docker containers and microservices, following the instructions defined in the standards [8] [9] [10] [11].

The SV-PMU microservice operation was evaluated using a laboratory testbed with an RTDS. Two methods for the evaluation of the TVE, FE and RFE behaviour of the PMUs were implemented. The first one is an evaluation in real-time using a Real-Time Automation Controller (RTAC) and the second one is an evaluation in offline mode using a Python Script.

Two versions of the SV-PMU microservice were implemented in the EPICS platform. The first one uses a two-cycle FIR filter, and the second one uses a one-cycle FIR filter.

The obtained test results indicate that the two versions of the SV-PMU microservice implemented in the EPICS platform performed well during the steady state and transient state tests, except in the steady state 10% current magnitude test. In this test, the maximum TVE of the current signals exceeded the TVE evaluation threshold. This occurs where the current magnitude is lower, and any deviation in current magnitude could result in significant deviations in the TVE of the currents. However, it should be noted that for the rest of the tests, the results obtained fully meet the standard requirements.

Regarding the measured latency, a better result was obtained in the implementation of the SV-PMU microservice using a one-cycle FIR filter compared to the implementation using a two-cycle FIR filter. It should be noted that the gain in latency has some side effects such as a worse rejection of noise due to a less aggressive filtering. The election of the filtering strategy is a well-known trade-off between latency and noise rejection, as stated in annex D.9 of the standard [8].

During the comparison of the performance of the SV-PMU microservice with the commercial PMU, it was observed that both PMUs obtained similar results in most of the testing scenarios. The worst TVEs were obtained during the steady state 10 % of rated current magnitude tests in both PMUs. The measured latency of the SV-PMU microservice using a one-cycle FIR filter (30.86 ms) is comparable to the measured latency of the commercial PMU (28.54 ms). The measured latency of the commercial PMU is less than 30ms, which indicates that the PMU algorithm it uses is different from the one implemented by the SV-PMU microservice using a one-cycle FIR filter. However, small differences in behaviour were observed between the PMUs in all tests executed.

The implementation of the SV-PMU microservice enhances the capabilities of the EPICS platform to operate as a Centralized Protection and Control system in Digital Substations, enabling it to be used as a vital part of WAMPAC systems. The SV-PMU microservice implemented during this work is a versatile microservice because it could manage at

> REPLACE THIS LINE WITH YOUR MANUSCRIPT ID NUMBER (DOUBLE-CLICK HERE TO EDIT) <

the same time multiple sampled values frames existent in the field, calculates all synchrophasors and finally serve to multiple PMU clients depending on their needs.

As part of future work, additional effort must be made to improve the performance of the *SV-PMU microservice* when dealing with low values of current magnitudes. The behaviour of the *SV-PMU microservice* will be evaluated using more than two instances of the microservice running in parallel, including additional protection and control microservices, in order to measure the worst-case latencies of the system as a whole. Additionally, an architecture with redundancy will be implemented and tested in terms of reliability and the results will be compared with the obtained by classical PMU units.

REFERENCES

- [1] N. George and O. D. Naidu, 'Distance protection issues with renewable power generators and possible solutions', in *16th International Conference on Developments in Power System Protection (DPSP 2022)*, Mar. 2022, pp. 373–378. doi: 10.1049/icp.2022.0969.
- [2] K. Jia, Z. Yang, T. Bi, and Y. Li, 'Impact of Inverter-Interfaced Renewable Energy Generators on Distance Protection and an Improved Scheme', in *2019 IEEE Power & Energy Society General Meeting (PESGM)*, Aug. 2019, pp. 1–1. doi: 10.1109/PESGM40551.2019.8973779.
- [3] S. Thengius, *Fault current injection from power electronic interfaced devices*. 2020. Accessed: Jan. 23, 2023. [Online]. Available: <http://um.kb.se/resolve?urn=urn:nbn:se:kth:diva-287728>
- [4] M. Debanjan and K. Karuna, 'An Overview of Renewable Energy Scenario in India and its Impact on Grid Inertia and Frequency Response', *Renewable and Sustainable Energy Reviews*, vol. 168, p. 112842, Oct. 2022. doi: 10.1016/j.rser.2022.112842.
- [5] L. Mehigan, D. Al Kez, S. Collins, A. Foley, B. Ó'Gallachóir, and P. Deane, 'Renewables in the European power system and the impact on system rotational inertia', *Energy*, vol. 203, p. 117776, Jul. 2020. doi: 10.1016/j.energy.2020.117776.
- [6] K. Jones *et al.*, 'Impact of Inverter Based Generation on Bulk Power System Dynamics and Short-Circuit Performance', IEEE PES Technical Report Number: PES-TR68, Jul. 2018.
- [7] L. Fanglei, W. Fan, Y. Jiaming, X. Guoyi, and B. Tianshu, 'Estimating Maximum Penetration Level of Renewable Energy Based on Frequency Stability Constrains in Power Grid', in *2020 5th Asia Conference on Power and Electrical Engineering (ACPEE)*, Jun. 2020, pp. 607–611. doi: 10.1109/ACPEE48638.2020.9136471.
- [8] 'IEEE/IEC International Standard - Measuring relays and protection equipment - Part 118-1: Synchrophasor for power systems - Measurements', *IEC/IEEE 60255-118-1:2018*, pp. 1–78, Dec. 2018. doi: 10.1109/IEEESTD.2018.8577045.
- [9] 'IEEE Standard for Synchrophasor Measurements for Power Systems', *IEEE Std C37.118.1-2011 (Revision of IEEE Std C37.118-2005)*, pp. 1–61, Dec. 2011. doi: 10.1109/IEEESTD.2011.6111219.
- [10] 'IEEE Standard for Synchrophasor Measurements for Power Systems – Amendment 1: Modification of Selected Performance Requirements', *IEEE Std C37.118.1a-2014 (Amendment to IEEE Std C37.118.1-2011)*, pp. 1–25, Apr. 2014. doi: 10.1109/IEEESTD.2014.6804630.
- [11] 'IEEE Standard for Synchrophasor Data Transfer for Power Systems', *IEEE Std C37.118.2-2011 (Revision of IEEE Std C37.118-2005)*, pp. 1–53, Dec. 2011. doi: 10.1109/IEEESTD.2011.6111222.
- [12] V. Terzija *et al.*, 'Wide-Area Monitoring, Protection, and Control of Future Electric Power Networks', *Proceedings of the IEEE*, vol. 99, no. 1, pp. 80–93, Jan. 2011. doi: 10.1109/JPROC.2010.2060450.
- [13] O. Tshenyego, R. Samikannu, and B. Mtengi, 'Wide area monitoring, protection, and control application in islanding detection for grid integrated distributed generation: A review', *Measurement and Control*, vol. 54, no. 5–6, pp. 585–617, May 2021. doi: 10.1177/0020294021989768.
- [14] D. Cai, L. Ding, X. Zhang, and V. Terzija, 'Wide area inter-area oscillation control system in a GB electric power system', *The Journal of Engineering*, vol. 2019, no. 16, pp. 3294–3300, 2019. doi: 10.1049/joe.2018.8752.
- [15] J. O'Brien *et al.*, 'Use of synchrophasor measurements in protective relaying applications', in *2014 67th Annual Conference for Protective Relay Engineers*, Mar. 2014, pp. 23–29. doi: 10.1109/CPRE.2014.6798992.
- [16] A. A. Prada Hurtado, E. Martínez Carrasco, M. T. Villén Martínez, and J. Saldana, 'Application of IIA Method and Virtual Bus Theory for Backup Protection of a Zone Using PMU Data in a WAMPAC System', *Energies*, vol. 15, no. 9, p. 3470, Jan. 2022. doi: 10.3390/en15093470.
- [17] C. Brunner, G. Lang, F. Leconte, and F. Steinhauser, 'Implementation guideline for digital interface to instrument transformers using IEC 61850-9-2', *Tech. Rep.*, 2004, [Online]. Available: https://iec61850.ucaiug.org/implementation%20guidelines/digif_spec_9-2le_r2-1_040707-cb.pdf
- [18] 'IEC 61850-9-2:2011+AMD1:2020 CSV | IEC Webstore | cyber security, smart city, LVDC'. Accessed: Feb. 01, 2024. [Online]. Available: <https://webstore.iec.ch/publication/66549>
- [19] GE Vernova, 'Measurement, Recording & Time Sync'. Accessed: Jan. 31, 2024. [Online]. Available: https://www.gegridsolutions.com/measurement_recording_timesync/catalog/rpv311.htm
- [20] SEL Inc, 'SEL Sampled Values (SV) Process Bus Solutions', selinc.com. Accessed: Jan. 31, 2024. [Online]. Available: <https://selinc.com/solutions/sampled-values/>
- [21] M. N. Agostini, L. B. de Oliveira, C. Dutra, S. L. Zimath, I. C. Decker, and A. Grid, 'Merging Unit Application for Synchronized Phasor Measurements', Accessed: Jan. 31, 2024. [Online]. Available: <http://www.truc.org/wp-content/uploads/TA-P5.pdf>
- [22] P. Castello, A. D. Femine, D. Gallo, M. Luiso, C. Muscas, and P. A. Pegoraro, 'Measurement of Synchrophasors with Stand Alone Merging Units: a Preliminary Study', in *2021 IEEE International Instrumentation and Measurement Technology Conference (I2MTC)*, May 2021, pp. 1–6. doi: 10.1109/I2MTC50364.2021.9460086.
- [23] G. Frigo and M. Agustoni, 'Phasor Measurement Unit and Sampled Values: Measurement and Implementation Challenges', in *2021 IEEE 11th International Workshop on Applied Measurements for Power Systems (AMPS)*, Sep. 2021, pp. 1–6. doi: 10.1109/AMPS50177.2021.9586036.
- [24] M. Agustoni, P. Castello, and G. Frigo, 'Phasor Measurement Unit With Digital Inputs: Synchronization and Interoperability Issues', *IEEE Transactions on Instrumentation and Measurement*, vol. 71, pp. 1–10, 2022. doi: 10.1109/TIM.2022.3175052.
- [25] 'Docker: Accelerated Container Application Development'. Accessed: Jan. 31, 2024. [Online]. Available: <https://www.docker.com/>
- [26] 'Plataforma EPICS: implementación flexible y escalable de sistemas automáticos', ELEWIT. Accessed: Sep. 14, 2022. [Online]. Available: <https://www.elewit.ventures/es/actualidad/plataforma-epics-implementacion-flexible-y-escalable-de-sistemas-automaticos>
- [27] A. A. Prada Hurtado, M. Manana, M. T. Villén Martínez, M. Á. Oliván Monge, E. M. Carrasco, and C. R. del Castillo, 'PMU Implementation Using IEC61850 Sampled Values Implemented in a CPC Platform', in *2024 IEEE 14th International Workshop on Applied Measurements for Power Systems (AMPS)*, Sep. 2024, pp. 1–6. doi: 10.1109/AMPS62611.2024.10706693.
- [28] F. Reghenzani, G. Massari, and W. Fornaciari, 'The Real-Time Linux Kernel: A Survey on PREEMPT_RT', *ACM Comput. Surv.*, vol. 52, no. 1, p. 18:1–18:36, Feb. 2019. doi: 10.1145/3297714.
- [29] K. Kurek, Ł. Nogal, R. Kowalik, and M. Januszewski, 'Implementation of IEC 61850 power protection tester in Linux environment', *Bulletin of the Polish Academy of Sciences. Technical Sciences*, vol. 68, no. 4, pp. 689–696, 2020.
- [30] M. T. Villen Martinez, M. P. Comech, A. A. P. Hurtado, M. A. Oliván, D. L. Cortón, and C. R. D. Castillo, 'Software-Defined Analog Processing Based on IEC 61850 Implemented in an Edge Hardware Platform to be Used in Digital Substations', *IEEE Access*, vol. 12, pp. 11549–11560, 2024. doi: 10.1109/ACCESS.2024.3354718.
- [31] M. T. Villen Martinez *et al.*, 'Description of an edge computing solution to be used in Digital Substations', in *2023 IEEE PES Innovative Smart Grid Technologies Europe (ISGT EUROPE)*, Oct. 2023, pp. 1–6. doi: 10.1109/ISGTEUROPE56780.2023.10408455.

> REPLACE THIS LINE WITH YOUR MANUSCRIPT ID NUMBER (DOUBLE-CLICK HERE TO EDIT) <

[32] M. T. Villen Martinez *et al.*, 'A computer-assisted Faulted Phase Selection Algorithm for dealing with the effects of Renewable Resources in Smart grids', *NEIS Conference on Sustainable Energy Supply and Energy Storage System*, pp. 192–197, Sep. 2023.

[33] G. Frigo, P. A. Pegoraro, and S. Toscani, 'Low-Latency, Three-Phase PMU Algorithms: Review and Performance Comparison', *Applied Sciences*, vol. 11, no. 5, Art. no. 5, Jan. 2021, doi: 10.3390/app11052261.

[34] 'IEC 61869-9:2016 | IEC Webstore'. Accessed: Feb. 01, 2024. [Online]. Available: <https://webstore.iec.ch/publication/24663>

[35] 'IEC 61869-13:2021 | IEC Webstore'. Accessed: Feb. 12, 2025. [Online]. Available: <https://webstore.iec.ch/en/publication/28359>

[36] SEL Inc, 'SEL-3555 Real-Time Automation Controller (RTAC) - Documentation', selinc.com. Accessed: Jan. 30, 2024. [Online]. Available: <https://selinc.com/products/3555/docs/>

[37] SEL Inc, 'SEL-5703 Synchrowave Monitoring Real-Time and Historic Trending and Archiving - Documentation', selinc.com. Accessed: Jan. 30, 2024. [Online]. Available: <https://selinc.com/products/5703/docs/>

[38] D. Gurusinghe, D. Ouellette, and R. Kuffel, 'An Automated Test Setup for Performance Evaluation of a Phasor Measurement Unit', Jun. 2016.

[39] S. S. Biswas, A. K. Srivastava, J. S. Park, and J. Castaneda, 'Tool for testing of phasor measurement units: PMU performance analyser', *IET Generation, Transmission and Distribution*, vol. 9, pp. 154–163, Jan. 2015, doi: 10.1049/iet-gtd.2014.0104.

[40] 'New Developments at RTDS Technologies'. Accessed: Feb. 01, 2024. [Online]. Available: https://site.ieee.org/winnipeg/files/2011/10/IEEE_PES_WPG_2011_1_018_Presentation-.pdf

[41] SEL Inc., 'ACCELERATOR RTAC@SEL-5033 Software, Instruction Manual 2020'. Schweitzer Engineering Laboratories, Inc., 2020. Accessed: Jan. 18, 2023. [Online]. Available: <https://selinc.com/es/products/5033/docs/>

[42] T. M. Antonsen, 'PLC Controls with Structured Text (ST), V3: IEC 61131-3 and best practice ST programming'. BoD – Books on Demand, 2020.

[43] SEL Inc., 'SEL RTAC Programming Reference 2021'. Schweitzer Engineering Laboratories, Inc., 2021. Accessed: Jan. 18, 2023. [Online]. Available: <https://selinc.com/es/products/5033/docs/>



Anibal Antonio Prada Hurtado. Electrical Engineer from Simón Bolívar University of Venezuela (2010) and holds an MSc in Renewable Energies from the Valencian International University of Spain (2023). He has been working at CIRCE technology center since 2018, where he is a Project Manager in the Infrastructure of Electric Grids group within the Electrical System area. He participates in R&D projects related to protection relays in transmission and distribution systems and WAMPAC systems applied to transmission grid. He has more than ten years of experience testing, commissioning, setting and installing protection relays for multiple manufacturers within the electrical industry. Currently, he is pursuing an industrial PhD in the area of WAMPAC systems.



Mario Manana. (Senior Member, IEEE). Full Professor of Electrical Engineering. He received the B.S. degree in telecommunications engineering from the University of Alcalá, Spain, in 1992 and the M.S. and Ph.D. degrees in telecommunications engineering from the University of Cantabria, Spain, in 1995 and 2000, respectively. From 2005 to 2012, he has been the head of the Department of Electrical and Energy Engineering, University of Cantabria (UC). From 2012 to 2016, he was the Director of the Sustainability Office attached to the vice-chancellor of Campus, Services, and Sustainability. From March 2016 to October 2024, he was Vice-Chancellor of Campus, Services, and Sustainability (UC). He also works as a Lecturer and Researcher with the Department of Electrical and Energy Engineering; he leads the Advanced Electro-Energetic Technology Group (GTEA) and from 2016 to 2019 the

Viesgo Energy Chair. His research interests include power quality, energy efficiency, and grid-integration of renewable energies.



Maria Teresa Villén Martínez. received the degree in Industrial Engineering with specialization in Electrical Systems in 2003, and the Ph.D. degree in Renewable Energies and Energy Efficiency in 2024, both from the University of Zaragoza. Since 2007, she has served as R&D Project Manager at the Research Centre for Energy Resources and Consumption (CIRCE) in Zaragoza, Spain, working on both EU-funded and nationally funded projects focused on power system protection relays, renewable energies integration, and smart grid.

Additionally, she has experience testing protection relays in laboratories and substations for various DSOs and manufacturers. Her main research interests include developing new protection algorithms for AC and DC grids and studying the integration of renewable energy sources and their potential impact on protection systems.



Miguel Angel Olivan. PhD and MsC from the University of Zaragoza. Twenty years of experience in software development focused mainly on data acquisition systems, signal processing, data analysis and Supervisory Control And Data Acquisition (SCADA) systems. His main role in CIRCE is the design and development of Smart Grids oriented software in the fields of data acquisition, measurements, signal processing, data analysis, automation, and Power Quality from Embedded and Edge to Cloud environments. Additionally, his role includes the design and implementation of Electric Vehicle and IEC 61850 (MMS, Sampled Values y GOOSE) software.



Eduardo Martínez Carrasco. received his M.S. in Industrial Engineering from the University of Zaragoza in 2011. He also has a M.S. in Electric and Electronic Engineering and Control Systems and he is PhD in Renewable Energies and Energy Efficiency, working in his thesis on improved distance protection algorithm in grids with high penetration of renewable energies. He has worked in CIRCE since 2011, where he is currently the Head of Power System Protection team. He is specialized in control system algorithms and

protection relay engineering applied both to short circuit and wide area protection.



Carlos Rodríguez Del Castillo received his Telecommunication Engineer degree from the Seville University of Engineers in 1997. After graduation Carlos moved to Madrid and joined ELIOP, S.A. in 1998 where he worked for seven years in SCADA development projects. Carlos has been involved in the design and implementation of multiple SCADA communication system solutions with legacy protocols and has a field experience in working with standards. In 2005 Carlos joined Redeia where he worked as a substation engineer

involved in IEC 61850 and legacy solutions for secondary systems until 2020, when he moved to Elewit, the innovation company of Redeia group. He is member of the IEC TC57 WG10.